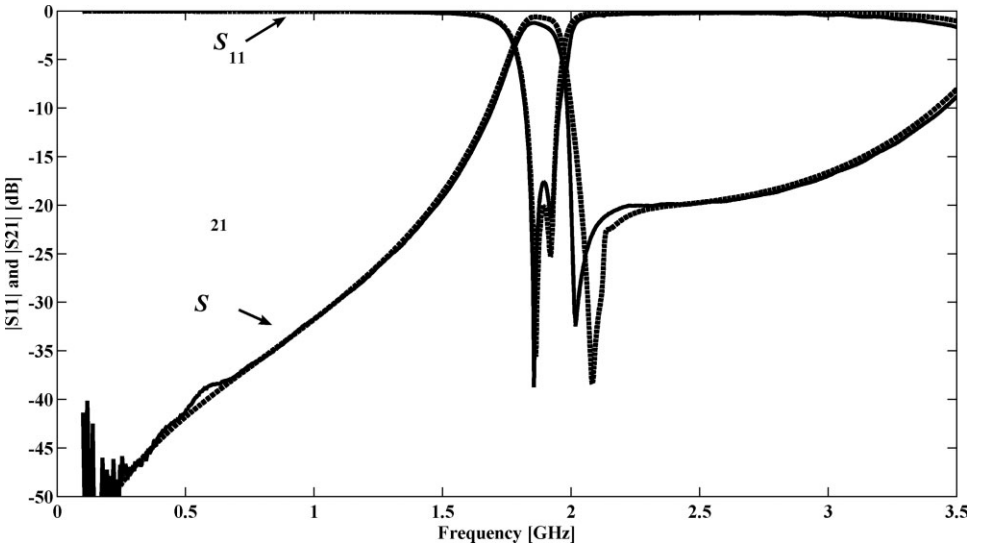

Figure 5 Measured (solid line) and simulated (dashed line) S_{11} and S_{21} parameters of the designed filter

mm. The strips of the three-line-microstrip section have a width of 1.4 mm and are separated a distance of 0.2 mm. The microstrip sections have a width of 4.6 mm to achieve a characteristic impedance of 50 Ω.

For the circuit simulation, the characteristic impedances and propagation constants of the ee, oo, and oe modes have been obtained from an electromagnetic analysis performed with Agilent™ Momentum. The via holes have been modeled using the model proposed in [8].

Figure 5 compares the measured and simulated [using the circuit model of Figure 4(b)] S_{11} and S_{21} parameters of the designed filter, showing a good agreement. The measured and simulated insertions losses are 1.2 and 0.7 dB, respectively. The measured and simulated bandwidths are 9.7 and 10.1%, respectively. The results validate both the multimodal approach and the filter structure proposed in this letter.

4. CONCLUSIONS

In this letter, a new two-pole compact BPF using an asymmetric short-circuited spurline resonator is presented. It has been analyzed by means of a new multimodal model for a microstrip to three-line-microstrip cross. This multimodal model provides a useful tool to parametrically study the dependence of the filter performance on its dimensions. Based on this parametric study, a series of design rules has been obtained, which allow a rapid fine tuning of the filter central frequency and bandwidth. Finally, a BPF with a 1.9-GHz center frequency has been designed, simulated, and measured. Simulations and measurements show a good agreement, and therefore, validate both the filter structure and its multimodal model.

ACKNOWLEDGMENTS

This work was supported by the Spanish Government under Project TEC2005-04238 (Ministerio de Educación y Ciencia).

REFERENCES

1. R. Schwindt and C. Nguyen, Spectral domain analysis of three symmetric coupled lines and application to a new band-pass filter, IEEE Trans Microwave Theory Tech 42 (1994), 1183–1189.
2. R. Schwindt and C. Nguyen, A new compact band-pass filter employing three parallel-coupled lines, IEEE MTT-S International Microwave Symposium Digest, San Diego, CA, (1994), 245–247.
3. C. Nguyen, New compact wideband band-pass filter using three parallel-coupled lines, Electron Lett 30 (1994), 2149–2150.
4. C. Nguyen, Miniaturized multi-octave band-pass filters, IEEE Antennas and Propagation Intternational Symposium, Newport Beach, CA, (1995), 1210–1213.
5. C. Nguyen, Microstrip spurline band-pass filters, IEEE Antennas Propag Int Symp, Orlando, FL, (1999), 206–209.
6. D. Pavlidis and H. L. Hartnagel, The design and performance of three-line-microstrip couplers, IEEE Trans Microwave Theory Tech 24 (1976), 631–640.
7. P. Rodriguez-Cepeda, M. Ribó, F.J. Pajares, J.R. Regué, A.M. Sánchez, and A. Pérez, Multimodal circuit model for the analysis of asymmetric shunt impedance transitions, IEEE EMC International Symposium, Detroit, MI, 2008.
8. M.E. Goldfarb and R.A. Pucel, Modeling via hole grounds in microstrip, IEEE Microwave Guided Wave Lett 1 (1991), 135–137.

RAYLEIGH ASSISTED BRILLOUIN EFFECTS IN DISTRIBUTED RAMAN AMPLIFIERS UNDER SATURATED CONDITIONS AT 40 Gb/s

M. T. M. Rocco Giraldi,[1] A. M. Rocha,[2] B. Neto,[2] C. Correia,[3] M. E. V. Segatto,[4] M. J. Pontes,[4] A. P. L. Barbero,[5] J. C. W. Costa,[6] M. A. G. Martinez,[7] O. Frazão,[3] J. M. Baptista,[3] H. M. Salgado,[3] M. B. Marques,[3] A. L. J. Teixeira,[2] and P. S. André[2]

[1] Electrical Engineering Department, IME, Rio de Janeiro, 22.290-270, Brazil; Corresponding author: mtmrocco@ime.eb.br
[2] Instituto de Telecomunicações, Aveiro, Portugal
[3] INESC Porto, Porto, Portugal
[4] Electrical Engineering Department, UFES, Vitória, Brazil
[5] Telecommunications Engineering Department, UFF, Niterói, Brazil
[6] Electrical Engineering Department, UFPA, Belém, Brazil
[7] Electronic Engineering Department, CEFET/RJ, Rio de Janeiro, Brazil

Received 31 July 2009

ABSTRACT: *This article analyzes experimentally the limitations observed in lightwave systems using distributed Raman amplifiers operating under large pump power input conditions. The Brillouin effect is observed as the pump power reaches 1 W. The presence of Brillouin peaks degrades the performance of the system. The Raman amplification*

occurs in single mode and dispersion compensating fibers, being evaluated in a link at transmission rate of 40 Gb/s. © 2010 Wiley Periodicals, Inc. Microwave Opt Technol Lett 52: 1331–1335, 2010; Published online in Wiley InterScience (www.interscience.wiley.com). DOI 10.1002/mop.25162

Key words: *stimulated Brillouin scattering; distributed Raman amplifier; Rayleigh scattering*

1. INTRODUCTION

Raman amplification is being actively studied as one of the key technologies for large capacity wavelength division multiplexing (WDM) networks [1–3]. Several reports [4, 5] of long haul transmission experiments show the use of C-band or L-band Raman amplification within the range from 1530.0 to 1610.0 nm because signal loss is the lowest in these bands. Further wavelength ranges such as U-, S- and O- bands are being explored to enlarge the huge bandwidth demand of WDM networks [6, 7].

A cost-effective alternative to improve the already installed long-haul system capacity is designing amplifiers that support higher number of input channels operating beyond the saturation [8]. The natural candidate to act as an efficient broadband amplifier in a high-capacity communication system is the distributed Raman amplifier (DRA). In such devices, it is possible to simultaneously compensate attenuation and group velocity dispersion with a dispersion compensating fiber (DCF). However, the implementation of Raman amplifiers requires multiple high pump power lasers. Therefore, the increased pump power available in the networks can lead to undesirable nonlinear effects. The stimulated Brillouin scattering (SBS) is one of the most important nonlinear effects in single mode fiber transmission systems, which employ narrow-linewidth single frequency lasers [9] and may lead to interchannel interference between counterpropagating signal waves in bidirectional transmission systems [10]. SBS was already reported in a specific configuration used in DRAs [11].

The continued Raman pump lasers evolution has enhanced the pump power and also reduced the spectral linewidth of such devices. It means to have a higher pump power density propagating into the fiber; therefore, the conditions to raise nonlinear effects such as SBS are achieved more easily. The observation of the Brillouin effect is because of an excessive optical power inside the fiber that leads to SBS sidebands. Obviously, no one would want to use such high power in a real system. However, if an all-Raman amplified system is being considered, the reduced linewidth of the ''state-of-the-art'' Raman pump lasers devices decreases, quite significantly, the threshold to observe such nonlinear effects. It means that further increase of the pump power could deeply degrade the system performance and disable its operation. Therefore, it is relevant to evaluate how those amplifiers behave under high pump power beyond the saturation.

When the Brillouin Stokes lines are assisted by Rayleigh scattering, multiwavelength fiber laser is obtained. For instance, Min et al. [12] proposed a multiwavelength fiber laser with flat amplitude equal spacing 798 channels. Park et al. [13, 14] have studied the dynamics of cascaded Brillouin-Rayleigh scattering in a DRA. Brillouin-Raman comb fiber laser with cooperative Rayleigh scattering in a linear cavity formed by high reflectivity element at both ends of the laser cavity was proposed by Zamzuri et al. [15]. Recently, an interrogation system using Raman fiber Bragg grating laser sensor with cooperative Rayleigh scattering was demonstrated [16].

This article presents the experimental analysis for the study of the Brillouin effect in a high-capacity communication system using DRA with one signal channel modulated at 40 Gb/s. To manage the optical link dispersion and to enhance the amplifier gain, DCF was combined with singlemode fiber (SMF-28).

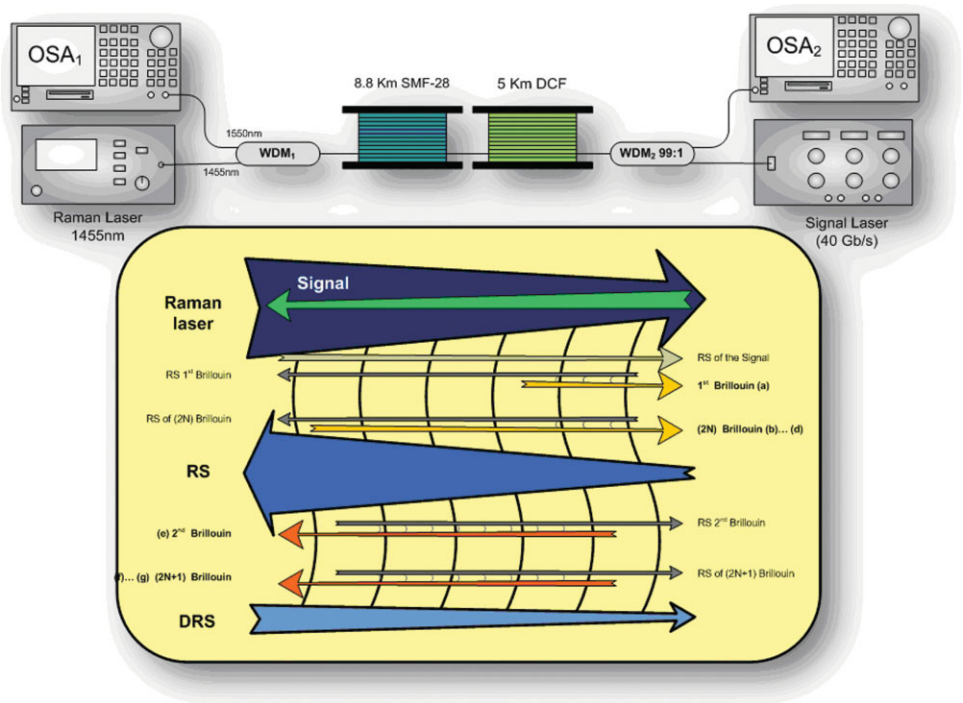

Figure 1 Configuration of the Raman amplifier with DCF + SMF-28 fibers set to the spectral evaluation of stimulated Brillouin scattering effect. RS, Rayleigh Scattering and DRS, Double Rayleigh Scattering. [Color figure can be viewed in the online issue, which is available at www.interscience.wiley.com]

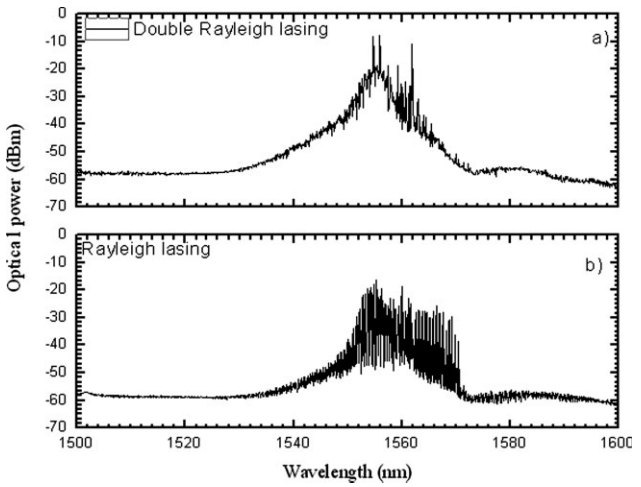

Figure 2 Rayleigh lasing generated by the distributed mirror: (A) DR lasing when is observed in Raman copropagating and (B) RS lasing when is observed in Raman counter propagating

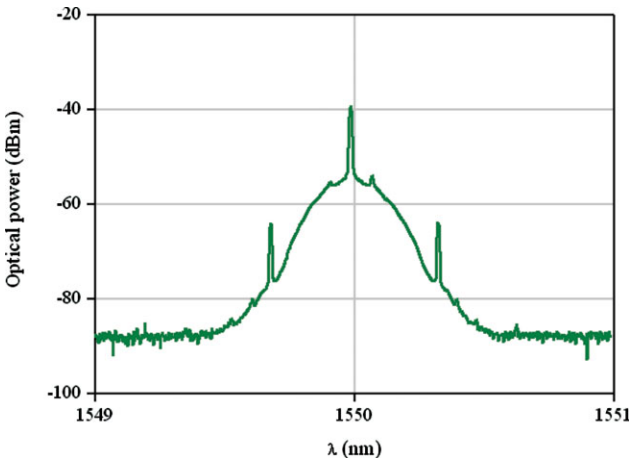

Figure 3 Signal output power as a function of signal wavelength under modulation rate of 40 Gb/s with no Raman pumping. [Color figure can be viewed in the online issue, which is available at www.interscience.wiley.com]

However, the results suggest that nonlinear effects induced mainly at the DCF are imposing limitations on the studied system. The main peaks measured at high pump power levels are attributed to SBS.

2. EXPERIMENTAL SETUP

In this work, two different configurations were evaluated using the setup of Figure 1, allowing the analysis of the transmitted and reflected signals. The signal channel at 1550.0 nm with a launched power of 10 dBm was modulated at 40 Gb/s and propagated through 13.8 km of optical fibers. The lengths of the SMF-28 and DCF were 8.8 and 5.0 km, respectively. The DCF presents a dispersion of −132 ps/nm.km. It used a highly pumped DRA with pump power of 1 W and pump wavelength of 1455 nm. The optical spectrum analyzers (OSAs) used presented resolution bandwidths of 0.7 nm.

The role of using a 40 Gb/s signal in the experiments is to enhance the transmission repetition rate considering fiber links with just tenths of kilometers. It means evaluating the trade-off between the Raman high pump power level used and the impairments generated by the high bit rate that can degrade the system performance.

For the transmission and reflection cases, Rayleigh assisted Brillouin-Stokes lines at ∼11 GHz are expected. For the transmission case, the Brillouin-Stokes even-order lines and the Rayleigh odd-order lines are obtained. For the reflection case, the Brillouin-Stokes odd-order lines and the Rayleigh even-order lines are obtained. It is also expected different amplitudes for Rayleigh components in the forward and backward directions, which are mainly attributed to the dependence of Raman gain efficiency on the pumping direction in the experimental setup.

3. RESULTS

Before injecting the signal in the setup configuration described in Figure 1, it was analyzed the response of the DCF when the Raman pump is injected. Figure 2 shows the response obtained when the Rayleigh scattering lasing is generated by the distributed mirror: (a) double Rayleigh scattering (DRS) lasing when is observed in Raman copropagating and (b) Rayleigh scattering (RS) lasing when is observed in Raman counterpropagating. The lasing is because of the distributed mirror created inside the DCF and corresponds to a similar effect such as the reflections

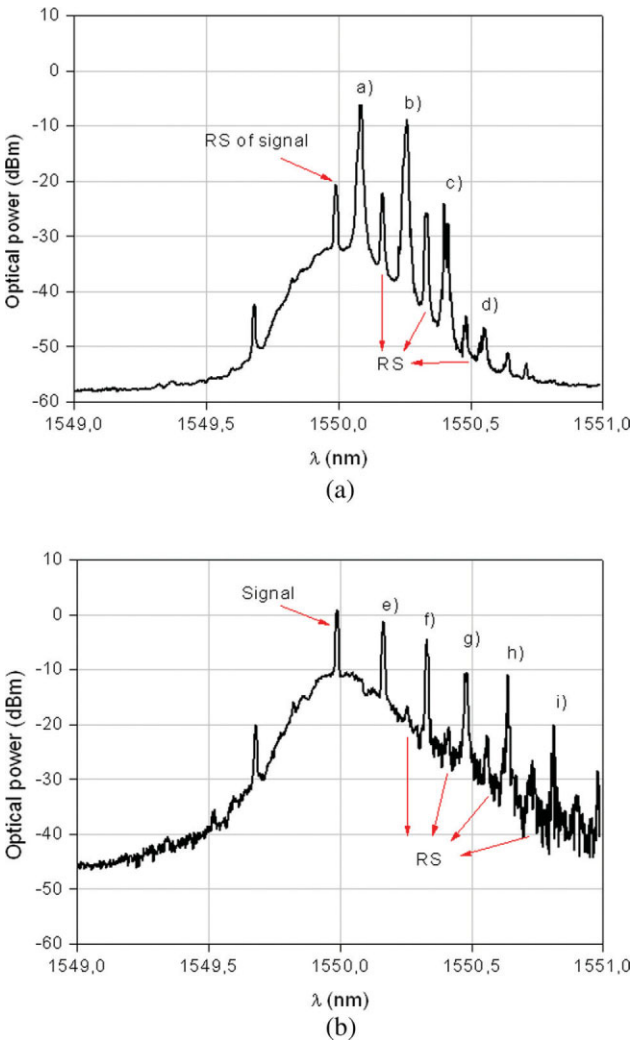

Figure 4 Signal output power as a function of signal wavelength under modulation rate of 40 Gb/s for a laser pump power of 1.0 W: (a) measured in the reflection configuration and (b) measured in the transmission configuration. [Color figure can be viewed in the online issue, which is available at www.interscience.wiley.com]

of two discrete mirrors with effective reflectance proportional to the ratio of the total backscattered to the incident power [17]. This distributed mirror appears when the Raman gain is very high. In this case, not only Rayleigh scattering is generated by the pump signal, but also this Rayleigh scattering generates the double Rayleigh scattering wave. The DRS signal with the amplified spontaneous emission of the Raman amplifier induces an incoherent multiple path interference, which is noise associated with the beating of multiple different delayed replicas of the signal itself (Fig. 2). The distributed mirror combined with the grating obtained by the acoustic wave forms a linear cavity where the Rayleigh assisted Brillouin Stokes lines are generated. This is a sequential cascaded process. The grating acoustic generated by the signal at 40 Gb/s works as a periodic filter with a frequency spacing of $\sim$10.5 GHz.

Figure 3 shows the signal output at 40 Gb/s without Raman pump applied in the setup of the Figure 1. A very small Brillouin peak appears around 1550 nm because of the nonlinear characteristics of the DCF.

Figure 4(a) shows the signal output modulated at 40 Gb/s after propagating over 8.8 km of SMF-28 plus 5.0 km of DCF, and measured with OSA 2 in the reflected configuration shown in Figure 1. In this case, the Raman amplifier pump laser introduces 1.0 W of pump power at the SMF-28 input. Peaks spaced by $\sim$0.2 nm ($\sim$10.5 GHz) can be observed from 1550 to 1550.7 nm. The separation of the peaks (Rayleigh assisted Brillouin Stokes lines) associated to the odd-orders correspond to the Brillouin-Stokes lines (peaks a–d) and the ones associated to the even-orders correspond to the Rayleigh scattering. In this case, the amplitude of the Brillouin peaks is similar because of the Raman gain efficiency on pumping direction. The output signal was also measured in the transmitted configuration, as shown in Figure 4(b). The peaks were also observed. But, there is no peak of Rayleigh scattering between the output signal and peak (e). The cascaded stimulated Brillouin is formed only by the even-order lines corresponding to the Brillouin-Stokes lines (peaks e–i) in cooperative with the Rayleigh scattering. The Rayleigh lines in this region are very faint because of the fact that stimulated Brillouin lines have been generated mostly at the first part of the DCF link, because of the high nonlinear properties of the fiber. After Peak (e), the separation is $\sim$10.5 GHz and we can see small peaks corresponding to the Rayleigh scattering of the odd-order lines associated to Brillouin-Stokes lines. Comparing the two figures [Fig. 4(a) and 4(b)], the Rayleigh assisted Brillouin-Stokes lines in Figure 4(b) have similar amplitude power. This is because of the cascaded stimulated Brillouin is counterpropagating with the Raman amplification and also because the Rayleigh lasing amplitude is uniform in the wavelength region of the Raman gain. Combining both effects with the input signal at 40 Gb/s, Rayleigh assisted Brillouin-Stokes lines are obtained. The transmission system performance can be strongly affected by those effects, as they appear as noise in the receiver and degrade the system signal-to-noise ratio by their multiple reflections propagating nature.

4. CONCLUSIONS

We have demonstrated a high-capacity Raman amplified system using one signal channel modulated by 40 Gb/s. We have also shown the limitations imposed by SBS to the system when extremely high pump power levels are involved. The high pump power of a laser presenting short spectral linewidth was sufficient to generate Brillouin sidebands, even when just one channel at a transmission rate of 40 Gb/s is injected in the system. The limitations are because of the DCF in the optical network. The DCF is necessary for enhancing the amplifier gain and compensating the dispersion in 40 Gb/s. However, for high pump power, the DCF behaves as a distributed mirror, which combined with the acoustic grating can form a linear cavity, and Rayleigh assisted Brillouin Stokes lines are obtained. In Summary, for the implemented set-up, with the distributed Raman amplification at 40 Gb/s, the power of the Raman pump cannot exceed 1 W.

ACKNOWLEDGMENTS

This work was supported in part by CNPq and GRICES under Grant 490695/2006-0. The authors greatly acknowledge the financial support provided by FCT through FEFOF (PTDC/EEA-TEL/72025/2006) and TECLAR (POCI/A072/2005) and CNPq (309049/2006-7 and 482657/2007-3) projects.

REFERENCES

1. M.N. Islam, Raman amplifiers for telecommunications: Physical principles, Springer series in optical sciences, Springer-Verlag, Berlin, Germany, 2003.
2. G.P. Agrawal, Nonlinear fiber optics, Academic Press, 1989.
3. O. Frazão, C. Correia, M.T.M. Rocco Giraldi, M.B. Marques, H.M. Salgado, M.A.G. Martinez, J.C.W.A. Costa, A.P. Barbero, and J.M. Baptista, Stimulated Raman scattering and its applications in optical communications and optical sensors, Open Opt J 3 (2009), 1–11.
4. H. Gnauck, G. Kaybon, S. Chandrasenknar, J. Leuthold, C. Doerr, and L. Stull, Proceedings Optical Fiber Communications Conference, vol. 1, Anaheim, CA, 2002, Postdeadline paper.
5. T. Matsuda, T. Kotanigawa, A. Naka, and T. Imai, 62 $\times$ 42.7 Gbit/s (2.5 Tbit/s) WDM signal transmission over 2200 km with broadband distributed Raman amplification, Electron Lett 38 (2002), 818–819.
6. T. Kotanigawa, T. Matsuda, and T. Kataoka, Applicable wavelength range of U-band signals in in-line Raman amplifier WDM systems, Electron Lett 39 (2003), 999–1000.
7. D. Sperti, P.S.André, B. Neto, A.M. Rocha, A. Bononi, F. da Rocha, and M. Facão, Experimental assessment of some Raman fiber amplifiers solutions for coarse wavelength division multiplexing applications, Photonic Netw Commun 16 (2008), 195–202.
8. S. Banerjee, A. Agarwal, D.F. Grosz, A.P. Kung, D.N. Maywar, M. Movassaghi, and T. Wood, Long-haul 64 $\times$ 40 Gbit/s DWDM transmission over commercial fibre types with large operating margins, Electron Lett 39 (2003), 92–94.
9. D. Cotter, Stimulated brillouin scattering in monomode optical fiber, J Opt Commun 4 (1983), 10–19.
10. R.G. Waarts and R.P. Braun, Crosstalk due to stimulated Brillouin scattering in monomode fibre, Electron Lett 21 (1985), 1114–1115.
11. M.I.M. Ali, A.K. Zamzuri, A. Ahmad, R. Mohamad, and M.A. Mahdi, Experimental validation of double-pass discrete Raman amplifier limitation for large signals, IEEE Photonics Technol Lett 18 (2006), 493–495.
12. B. Min, P. Kim, and N. Park, Flat amplitude equal spacing 798-channel Rayleigh-assisted Brillouin/Raman multiwavelength comb generation in dispersion compensating fiber, IEEE Photonics Technol Lett 13 (2001), 1352–1354.
13. K.D. Park, B. Min, P. Kim, N. Park, J.H. Lee, and J.S. Chang, Dynamics of cascaded Brillouin-Rayleigh scattering in a distributed fiber Raman amplifier, Opt Lett 27 (2002), 155–157.
14. K.D. Park, H. Ryu, W.K. Lee, S.K. Kim, H.S. Moon, and H.S. Suh, Threshold features of a Brillouin Stokes comb generated in a distributed fiber Raman amplifier, Opt Lett 28 (2003), 1311–1313.
15. A.K. Zamzuri, M.I.M. Ali, A. Ahmad, R. Mohamad, and M.A. Mahdi, Brillouin-Raman comb fiber laser with cooperative Rayleigh scattering in a linear cavity, Opt Lett 31 (2006), 918–920.

16. O. Frazão, C. Correia, J.M. Baptista, and J.L. Santos, Raman fibre Bragg-grating laser sensor with cooperative Rayleigh scattering for strain-temperature measurement, Meas Sci Technol 20 (2009), 1–5.
17. J.L. Gimlett, M.Z. Iqbal, N.K. Cheung, A. Righetti, F. Fontana, and G. Grass, Observation of equivalent Rayleigh scattering mirrors in lightwave systems with optical amplifiers, IEEE Photon Technol Lett 2 (1990), 211–213.

FULL-DUPLEX OFDM-ROF ARCHITECTURE BASED ON MILLIMETER-WAVE GENERATED BY OPTICAL PHASE MODULATOR

Yao Tao,[1] Lin Chen,[2] and Satoshi Goto[1]
[1] Department of System LSI, Graduate School of Information, Production and Systems, Waseda University, 2-7 Hibikino, Wakamatsu-ku, Kitakyushu-shi, Fukuoka 808-0135, Japan; Corresponding author: taoyao@gmail.com
[2] Key Laboratory for Micro/Nano Opto-Electronic Devices of Ministry of Education, School of Computer and Communication, Hunan University, Changsha 410082, China

Received 7 August 2009

ABSTRACT: *We proposed and experimentally demonstrate a bidirectional orthogonal frequency-division multiplexing-radio-over-fiber (OFDM-ROF) system by using an optical phase modulator and a fiber Bragger gating (FBG) to generate millimeter-wave. The downstream date is 2.5-Gb/s OFDM signals and the downstream wavelength is reused without signal erasure.* © 2010 Wiley Periodicals, Inc.
Microwave Opt Technol Lett 52: 1335–1337, 2010; Published online in Wiley InterScience (www.interscience.wiley.com). DOI 10.1002/mop.25175

Key words: *radio-over-fiber; orthogonal frequency-division multiplexing; full duplex; fiber Bragger gating; optical phase modulation*

1. INTRODUCTION

Optical orthogonal frequency-division multiplexing (OOFDM), which takes the advantages from its high spectral efficiency and the resistance to variety dispersions including chromatic dispersion (CD) and polarization-mode dispersion (PMD), has attracted great attention in long distance optical network domain. The broadband radio-over-fiber (ROF) system based on OOFDM technique becomes a hot research topic recently. The generation of millimeter (mm)-wave must be a key technique for ROF system [1–8]. Many researches on the generation of mm-wave by using external intensity modulator (IM) have been proposed. However, IM suffers from a flaw that the output of it is interrelated with the stability of the electrical circuit for DC bias [3, 4]. On the other hand, optical phase modulator (PM) which takes the advantages of small insertion loss and no DC bias can generate optical mm-wave with high optical signal-to-noise ratio and higher stability. Moreover, the output optical signals amplitudes of PM are constant, and only the relative output phase varies [5]. In this article, we proposed and experimentally demonstrated a ROF architecture in which the mm-wave is generated by using PM and fiber bragger gating (FBG) [6]. The downstream signal is 2.5-Gb/s OFDM signals and the wavelength of downlink is reused for uplink without the erasure of the downstream signals.

2. SYSTEM ARCHITECTURE AND EXPERIMENTAL SETUP

The architecture of whole full-duplex OFDM-ROF system is shown in Figure 1. The input continuous lightwave is modulated by using a PM based on double sideband modulation (DSB) scheme. A FBG is used to remove the optical central carrier, and then the mm-wave will be generated by beating the two peaks of the first-mode. The downstream OFDM signal is driven on the mm-wave by using an IM. Then this downstream OFDM signal is transmitted over a long distance fiber and is halved by using an optical coupler (OC). One part is used to provide wireless ROF service. This part of signals are converted to electrical signals by a high speed PIN detector and boosted by an electrical narrowband amplifier before it is broadcast by an antenna. At the receive part, the converted electrical signals are directly down-converted with LO signals by using an electrical mixer to retrieve the downstream OFDM signal, then the demodulation and analysis of OFDM signals are realized by an offline program and sent back by antenna. The other part of signals from OC is reused for uplink after suppressed a sideband of the optical downstream signal by using an interleaver (IL). The upstream date with 2.5-Gb/s OOK-NRZ signals which is received by antenna is driven on the reused lightwave by using another IM without the erasure of OFDM signals of the downstream lightwave. After transmitted over a long distance fiber, the upstream data is retrieved by using an optical receiver.

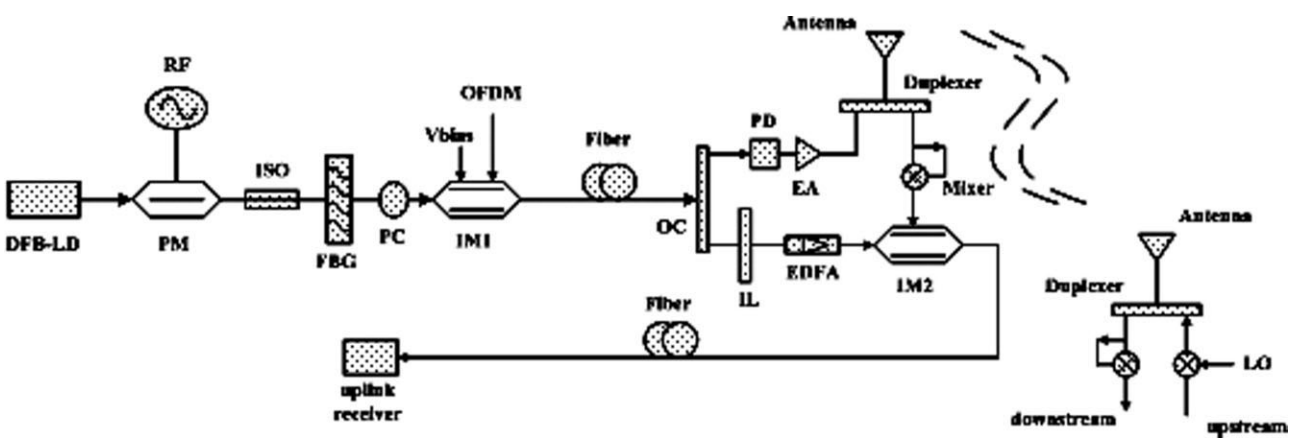

Figure 1 Principle of full-duplex OFDM-ROF system based on millimeter-wave generated by optical phase modulator. IL, interleave; IM, intensity modulator; PC, polarization controller; EA, electrical amplifier; OC, optical coupler